

Investigation of hidden-charm pentaquarks with strangeness $S = -1$

Xiaohuang Hu · Jialun Ping

the date of receipt and acceptance should be inserted later

Abstract Recently, a new hidden-charm pentaquark state $P_{cs}(4459)$ was reported by the LHCb Collaboration. Stimulated by the fact that all hidden-charm pentaquark states in $S = 0$ systems were successfully studied by the chiral quark model, we extended this study to the $S = -1$ systems. All possible states with quantum numbers $IJ^P = 0(\frac{1}{2})^-, 0(\frac{3}{2})^-, 0(\frac{5}{2})^-, 1(\frac{1}{2})^-, 1(\frac{3}{2})^-$ and $1(\frac{5}{2})^-$ have been investigated. The calculation results shows that the newly observed state $P_{cs}(4459)$ can be explained as $\Xi_c \bar{D}^*$ molecular state and the quantum numbers are $0(\frac{1}{2})^-$. In addition, we also find other molecular states $\Xi_c \bar{D}$, $\Xi_c^* \bar{D}$ and $\Xi_c' \bar{D}^*$. It is worth mentioning that $\Xi_c \bar{D}^*$ can form a two-peak structure from states in system $0(\frac{1}{2})^-$ and $0(\frac{3}{2})^-$. The decay width of all molecular states is given with the help of real scaling method. These hidden-charm pentaquark states is expected to be further verified in future experiments.

PACS 13.75.Cs · 12.39.Pn · 12.39.Jh

1 Introduction

Since Θ^+ was proposed in 2003 [1,2], the search of pentaquark states has always been a hot topic. A large number of exotic hadronic states, “XYZ” states which associated with tetraquark, have been discovered in experiments over the past decade. Naturally the observation of pentaquark state is expected. The important and prominent event arrived in 2015, the P_c^+ states $P_c^+(4380)$ and $P_c^+(4450)$, which are the strongest candidates for pentaquark states were observed by the LHCb

Collaboration in the $J/\psi p$ invariant mass spectrum of decay channel $\Lambda_b \rightarrow J\psi p K$ [3]. And then in 2019, the LHCb Collaboration reanalysed the same process with more data and updated their results, which shows that $P_c^+(4450)$ can split into two structures, $P_c^+(4440)$ and $P_c^+(4457)$, while $P_c^+(4312)$ is identified as a new structure [4]. These P_c^+ states all have a common feature that they are very close to baryon-meson thresholds, which led to one of the most popular interpretation of these P_c^+ states as molecular states [5,6,7,8,9,10,11]. Other possible explanations also exist, such as the compact pentaquark states [12,13]. In addition, the decay properties and width of these P_c^+ states also have been investigated in Ref. [14].

Very recently, the LHCb Collaboration reported a new pentaquark state with strangeness, $P_{cs}^+(4459)$ in the $J/\psi \Lambda$ invariant mass spectrum of decay channel $\Xi_b \rightarrow J\psi K^- \Lambda$ [15]. The mass and decay width of $P_{cs}^+(4459)$ are,

$$M = 4458.8 \pm 2.9_{-1.1}^{+4.7} \text{ MeV},$$
$$\Gamma = 17.3 \pm 6.0_{-5.7}^{+8.0} \text{ MeV},$$

while its spin and parity are unknown. Like other P_c^+ pentaquark states, the mass of $P_{cs}^+(4459)$ is very close to threshold of $\Xi_c \bar{D}^*$. Thus, some phenomenological models have been used to investigate whether $P_{cs}^+(4459)$ can be explained as a $\Xi_c \bar{D}^*$ molecular state, such as QCD sum rule [16,17], coupled channel unitary approach [18], effective field theory [19] and so on [20, 21,22,23]. Other structures of P_{cs} are also proposed, for example, diquark-diquark-antiquark structure [24]. Actually, there are many theoretical work on P_{cs} state before the experiment [25,26,27,28].

It is important to highlight here that, before the LHCb’s discovered several P_c^+ pentaquark states, their existence was predicted [29,30,31], and our quark model

Corresponding author: jlping@njnu.edu.cn

Department of Physics and Jiangsu Key Laboratory for Numerical Simulation of Large Scale Complex Systems, Nanjing Normal University, Nanjing 210023, P. R. China

calculation also gave a good description and prediction [32]. $P_c^+(4312)$, $P_c^+(4440)$ and $P_c^+(4459)$ were described as baryon-meson molecular states with the $IJ^P = \frac{1}{2}(\frac{1}{2})^- \Sigma_c \bar{D}$, $\frac{1}{2}(\frac{1}{2})^- \Sigma_c \bar{D}^*$ and $\frac{1}{2}(\frac{3}{2})^- \Sigma_c \bar{D}^*$, respectively. A lot of subsequent theoretical work also supports our conclusion [9,10,11,33]. Thus, it is natural to extend herein such study from P_c states to the P_{cs} states. Since the quark model was proposed by M. Gell-Mann and G. Zweig in 1964 respectively [34,35], it has become the most common approach to study the multi-quark system as it evolves. In this work, the constituent chiral quark model (ChQM) will still be employed to investigate $qqsc\bar{c}$ systems (q stands for u or d) corresponding to P_{cs} states. To calculate accurately the results of each possible system, Gaussian expansion method (GEM) [36], an accurate and universal few-body calculation method is adopted. The GEM is very suitable for the calculation of few-body systems. Within this method, the orbital wave functions of all relative motions of the systems are expanded by gaussians. After considering all possible configuration of color, spin and flavor degrees of freedom, we can identify the structures of the system. Finally, with the help of “real scaling method”, we can confirm the genuine five-quark resonances and their respective decay widths along.

The paper is organized as follow. After introduction, details of ChQM and GEM are introduced in Section II. In Section III, we present the method of finding and calculating the decay width of the genuine resonance state (“real scaling method”), and then we show the results with analysis and discussion of P_{cs} structure. Finally, We give a brief summary of this work in the last section.

2 CHIRAL QUARK model and wave functions

In this paper, ChQM is employed to investigate the P_{cs} states. The model has become one of the most common approaches to describe hadron spectra, hadron-hadron interactions and multi-quark states [37]. In this model, in addition to one-gluon exchange (OGE), the massive constituent quarks also interact with each other through Goldstone boson exchange. Besides, the color confinement and the scalar σ meson (chiral partner, acting on u and d quark only) exchange are also introduced. More details of this model can be found in Ref. [37,38]. The Hamiltonian of ChQM is given as fol-

lows:

$$H = \sum_{i=1}^n \left(m_i + \frac{p_i^2}{2m_i} \right) - T_{CM} + \sum_{j>i=1}^n V_{ij} \quad (1)$$

$$V_{ij} = V_{ij}^C + V_{ij}^G + V_{ij}^\chi + V_{ij}^\sigma, \quad (2)$$

$$V_{ij}^C = \boldsymbol{\lambda}_i^c \cdot \boldsymbol{\lambda}_j^c [-a_c(1 - e^{-\mu_c r_{ij}}) + \Delta], \quad (3)$$

$$V_{ij}^G = \frac{\alpha_s}{4} \boldsymbol{\lambda}_i^c \cdot \boldsymbol{\lambda}_j^c \left[\frac{1}{r_{ij}} - \frac{1}{6m_i m_j} \boldsymbol{\sigma}_i \cdot \boldsymbol{\sigma}_j \frac{e^{-r_{ij}/r_0(\mu)}}{r_{ij} r_0^2(\mu)} \right], \quad (4)$$

$$r_0(\mu) = \hat{r}_0/\mu, \quad \alpha_s = \frac{\alpha_0}{\ln\left(\frac{\mu^2 + \mu_0^2}{\Lambda_0^2}\right)}. \quad (5)$$

$$V_{ij}^\chi = v_\pi(\mathbf{r}_{ij}) \sum_{a=1}^3 \lambda_i^a \lambda_j^a + v_K(\mathbf{r}_{ij}) \sum_{a=4}^7 \lambda_i^a \lambda_j^a + v_\eta(\mathbf{r}_{ij}) [\cos \theta_P (\lambda_i^8 \lambda_j^8) - \sin \theta_P], \quad (6)$$

$$v_{ij}^\chi = \frac{g_{ch}^2}{4\pi} \frac{m_\chi^2}{12m_i m_j} \frac{\Lambda_\chi^2}{\Lambda_\chi^2 - m_\chi^2} m_\chi \left[Y(m_\chi r_{ij}) - \frac{\Lambda_\chi^3}{m_\chi^3} Y(\Lambda_\chi r_{ij}) \right] (\boldsymbol{\sigma}_i \cdot \boldsymbol{\sigma}_j), \quad (7)$$

$$\chi = \pi, K, \eta, \quad (8)$$

$$V_{ij}^\sigma = -\frac{g_{ch}^2}{4\pi} \frac{\Lambda_\sigma^2 m_\sigma}{\Lambda_\sigma^2 - m_\sigma^2} \left[Y(m_\sigma r_{ij}) - \frac{\Lambda_\sigma}{m_\sigma} Y(\Lambda_\sigma r_{ij}) \right]. \quad (9)$$

where T_{cm} is the kinetic energy of the center-of mass motion and μ is the reduced mass between two interacting quarks. Only the central parts of the interactions are given here because we are interested in the low-lying states of the multi-quark system. $\boldsymbol{\sigma}$ represents the SU(2) Pauli matrices; $\boldsymbol{\lambda}^c$ and $\boldsymbol{\lambda}$ represent the SU(3) color and flavor Gell-Mann matrices respectively; α_s denotes the strong coupling constant of one-gluon exchange and $Y(x)$ is the standard Yukawa functions. Because it is difficult to use the same set of parameters to have a good description of baryon and meson spectra simultaneously, we treat the strong coupling constant of one-gluon exchange with different values for quark-quark and quark-antiquark interacting pairs.

The model parameters are listed in Table I, and the calculated baryon and meson masses are presented in the Table II with the experimental values. From the calculation, most of the results are close to experimental values except for the A_c and J/ψ . In the follow-up calculation, we find that the molecular state corresponding to these two hadrons are open channels and these calculation errors do not cause mass inversion, so these errors do not affect our final results.

In the following, the wave functions for the five-quark systems are constructed and the eigen-energy is obtained by solving the Schrödinger equation. The wave function of the system consists of four parts: orbital, spin, flavor and color. The wave function of each part is

Table 1 Quark model parameters

Quark masses	$m_u = m_d$ (MeV)	313
	m_s (MeV)	555
	m_c (MeV)	1780
Goldstone bosons	$\Lambda_\pi = \Lambda_\sigma$ (fm $^{-1}$)	4.20
	$\Lambda_\eta = \Lambda_K$ (fm $^{-1}$)	5.20
	m_π (fm $^{-1}$)	0.70
	m_K (fm $^{-1}$)	2.51
	m_η (fm $^{-1}$)	2.77
	m_σ (fm $^{-1}$)	3.42
	$g_{ch}^2/(4\pi)$	0.54
	θ_F (°)	-15
Confinement	a_c (MeV)	280.3
	μ_c (fm $^{-1}$)	0.863
	Δ (MeV)	115.0
OGE	\hat{r}_0 (MeV fm)	49.3
	α_{uu}	0.623/0.924
	α_{us}	0.915/-
	α_{uc}	0.900/0.765
	α_{sc}	0.710/0.633
	α_{cc}	-/0.5

Table 2 The masses of ground-state baryons and mesons(unit: Mev)

	Λ	Σ	Σ^*	Λ_c	Σ'_c	Σ_c^*
CHQM	1114	1243	1404	2184	2453	2529
Expt	1116	1189	1385	2286	2455	2520
	Ξ_c	Ξ'_c	Ξ_c^*			
CHQM	2460	2580	2653			
Expt	2471	2589	2645			
	π	ρ	D	D^*	D_s	D_s^*
CHQM	140	698	1858	2023	1964	2156
Expt	140	775	1864	2007	1968	2112
	η_c	J/ψ				
CHQM	2984	3182				
Expt	2984	3097				

constructed in two steps, first construct the wave function of three-quark cluster and quark-antiquark cluster, respectively, then coupling two clusters wave functions to form the complete five-body one. In the following, the wave functions for $(qqs)(\bar{c}c)$ configuration is written down, the wave functions for other configuration can be obtained by exchange the indices of particles. The indices of particles q, q, s, \bar{c}, c are 1,2,3,4,5. The wave functions for $(qqc)(\bar{c}s)$ are obtained by exchange the particle indices 3 \leftrightarrow 5 as an example.

The first part is orbital wave function. A five-body system have four relative motions so it is written as follows.

$$\psi_{LM_L}^x = \left[\left[\left[\psi_{n_1 l_1}(\boldsymbol{\rho}) \psi_{n_2 l_2}(\boldsymbol{\lambda}) \right]_l \psi_{n_3 l_3}(\mathbf{r}) \right]_{l'} \psi_{n_4 l_4}(\mathbf{R}) \right]_{LM_L}, \quad (10)$$

where the Jacobi coordinates are defined as follows,

$$\begin{aligned} \boldsymbol{\rho} &= \mathbf{x}_1 - \mathbf{x}_2, \\ \boldsymbol{\lambda} &= \left(\frac{m_1 \mathbf{x}_1 + m_2 \mathbf{x}_2}{m_1 + m_2} \right) - \mathbf{x}_3, \\ \mathbf{r} &= \mathbf{x}_4 - \mathbf{x}_5, \\ \mathbf{R} &= \left(\frac{m_1 \mathbf{x}_1 + m_2 \mathbf{x}_2 + m_3 \mathbf{x}_3}{m_1 + m_2 + m_3} \right) - \left(\frac{m_4 \mathbf{x}_4 + m_5 \mathbf{x}_5}{m_4 + m_5} \right). \end{aligned} \quad (11)$$

\mathbf{x}_i is the position of the i -th particle. Then we use a set of gaussians to expand the radial part of the orbital wave function which is shown below,

$$\psi_{lm}(\mathbf{r}) = \sum_{n=1}^{n_{max}} c_{nl} \phi_{nlm}^G(\mathbf{r}) \quad (12)$$

$$\phi_{nlm}^G(\mathbf{r}) = N_{nl} r^l e^{-\nu_n r^2} Y_{lm}(\hat{\mathbf{r}}) \quad (13)$$

where N_{nl} is the normalization constant,

$$N_{nl} = \left(\frac{2^{l+2} (2\nu_n)^{l+3/2}}{\sqrt{\pi} (2l+1)!!} \right)^{\frac{1}{2}}, \quad (14)$$

and c_{nl} is the variational parameter, which is determined by the dynamics of the system. The Gaussian size parameters are chosen according to the following geometric progression:

$$\nu_n = \frac{1}{r_n^2}, r_n = r_{min} a^{n-1}, a = \left(\frac{r_{max}}{r_{min}} \right)^{\frac{1}{n_{max}-1}}, \quad (15)$$

where n_{max} is the number of Gaussian functions, and n_{max} is determined by the convergence of the results. In the present calculation, $n_{max} = 8$.

The details of constructing flavor, color and spin wave functions of 5-quark system can be found in Ref. [39], only the last expressions are shown here.

Flavor wave functions:

$$\begin{aligned} |\chi_{0,0}^{f1}\rangle &= \frac{1}{\sqrt{2}} (uds\bar{c}c - dus\bar{c}c) \\ |\chi_{0,0}^{f2}\rangle &= uus\bar{c}c \end{aligned} \quad (16)$$

Color wave functions:

$$\begin{aligned}
|\chi^{c1}\rangle &= \frac{1}{\sqrt{18}}(rgb - rbg + gbr - grb + brg - bgr) \\
&\quad (\bar{r}r + \bar{g}g + \bar{b}b) \\
|\chi^{c2}\rangle &= \frac{1}{\sqrt{192}} [2(2rrg - rgr - grr)\bar{r}b \\
&\quad + 2(rgg + grg - 2ggr)\bar{g}b \\
&\quad - 2(2rrb - rbr - brr)\bar{r}g - 2(rbb + brb - 2bbr)\bar{b}g \\
&\quad + 2(2ggb - gbg - bgg)\bar{g}r + 2(gbb + bgb - 2bbg)\bar{b}r \\
&\quad + (rbg - gbr + brg - bgr)(2\bar{b}b - \bar{r}r - \bar{g}g) \\
&\quad + (2rgb - rbg + 2grb - gbr - brg - bgr)(\bar{r}r - \bar{g}g)] \\
|\chi^{c3}\rangle &= \frac{1}{24} [6(rgr - grr)\bar{r}b + 6(rgg - grg)\bar{g}b \quad (17) \\
&\quad - 6(rbr - brr)\bar{r}g - 6(rbb - brb)\bar{b}g \\
&\quad + 6(gbg - bgg)\bar{g}r + 6(gbb - bgb)\bar{b}r \\
&\quad + 3(rbg + gbr - brg - bgr)(\bar{r}r - \bar{g}g) \\
&\quad + (2rgb + rbg - 2grb - gbr - brg + bgr) \\
&\quad (2\bar{b}b - \bar{r}r - \bar{g}g)]
\end{aligned}$$

Spin wave functions:

$$\begin{aligned}
|\chi_{\frac{1}{2},\frac{1}{2}}^{\sigma 1}\rangle &= \frac{1}{\sqrt{12}}(2\alpha\alpha\beta\alpha\beta - 2\alpha\alpha\beta\beta\alpha + \alpha\beta\alpha\beta\alpha \\
&\quad - \alpha\beta\alpha\alpha\beta + \beta\alpha\alpha\beta\alpha - \beta\alpha\alpha\alpha\beta) \\
|\chi_{\frac{1}{2},\frac{1}{2}}^{\sigma 2}\rangle &= \frac{1}{2}(\alpha\beta\alpha\alpha\beta - \alpha\beta\alpha\beta\alpha + \beta\alpha\alpha\beta\alpha - \beta\alpha\alpha\alpha\beta) \\
|\chi_{\frac{1}{2},\frac{1}{2}}^{\sigma 3}\rangle &= \frac{1}{6}(2\alpha\alpha\beta\alpha\beta + 2\alpha\alpha\beta\beta\alpha - \alpha\beta\alpha\alpha\beta - \alpha\beta\alpha\beta\alpha \\
&\quad - \beta\alpha\alpha\beta\alpha - \beta\alpha\alpha\alpha\beta - 2\alpha\beta\beta\alpha\alpha - 2\beta\alpha\beta\alpha\alpha \\
&\quad + 4\beta\beta\alpha\alpha\alpha) \\
|\chi_{\frac{1}{2},\frac{1}{2}}^{\sigma 4}\rangle &= \frac{1}{\sqrt{12}}(\alpha\beta\alpha\alpha\beta + \alpha\beta\alpha\beta\alpha - \beta\alpha\alpha\alpha\beta - \beta\alpha\alpha\beta\alpha \\
&\quad + 2\beta\alpha\beta\alpha\alpha - 2\alpha\beta\beta\alpha\alpha) \quad (18) \\
|\chi_{\frac{1}{2},\frac{1}{2}}^{\sigma 5}\rangle &= \frac{1}{\sqrt{18}}(3\alpha\alpha\alpha\beta\beta - \alpha\alpha\beta\alpha\beta - \alpha\alpha\beta\beta\alpha \\
&\quad - \alpha\beta\alpha\alpha\beta - \alpha\beta\alpha\beta\alpha - \beta\alpha\alpha\alpha\beta - \beta\alpha\alpha\beta\alpha \\
&\quad + \beta\beta\alpha\alpha\alpha + \beta\alpha\beta\alpha\alpha + \alpha\beta\beta\alpha\alpha) \\
|\chi_{\frac{3}{2},\frac{3}{2}}^{\sigma 1}\rangle &= \frac{1}{\sqrt{6}}(2\alpha\alpha\beta\alpha\alpha - \alpha\beta\alpha\alpha\alpha - \beta\alpha\alpha\alpha\alpha) \\
|\chi_{\frac{3}{2},\frac{3}{2}}^{\sigma 2}\rangle &= \frac{1}{\sqrt{2}}(\alpha\beta\alpha\alpha\alpha - \beta\alpha\alpha\alpha\alpha) \\
|\chi_{\frac{3}{2},\frac{3}{2}}^{\sigma 3}\rangle &= \frac{1}{\sqrt{2}}(\alpha\alpha\alpha\alpha\beta - \alpha\alpha\alpha\beta\alpha) \\
|\chi_{\frac{3}{2},\frac{3}{2}}^{\sigma 4}\rangle &= \frac{1}{\sqrt{30}}(2\alpha\alpha\beta\alpha\alpha + 2\alpha\beta\alpha\alpha\alpha + 2\beta\alpha\alpha\alpha\alpha \\
&\quad - 3\alpha\alpha\alpha\alpha\beta - 3\alpha\alpha\alpha\beta\alpha) \\
|\chi_{\frac{5}{2},\frac{5}{2}}^{\sigma 1}\rangle &= \alpha\alpha\alpha\alpha\alpha,
\end{aligned}$$

where χ^{c1} represents the color wave function of a color singlet-singlet structure, χ^{c2} and χ^{c3} represent the color

octet-octet wave functions respectively. The subscripts of χ_{I,I_z}^f (χ_{S,S_z}^σ) are total isospin (spin) and its third projection.

Finally, the total wave function of the five-quark system is written as:

$$\Psi_{JM_J}^{i,j,k} = \mathcal{A} \left[[\psi_L \chi_S^{\sigma_i}]_{JM_J} \chi_j^{fi} \chi_k^{ci} \right], \quad (19)$$

where the \mathcal{A} is the antisymmetry operator of the system which guarantees the antisymmetry of the total wave functions when identical particles exchange. Under our numbering scheme, the antisymmetry operator is

$$\mathcal{A} = 1 - (12) \quad (20)$$

At last, we solve the following Schrödinger equation to obtain eigen-energies of the system,

$$H\Psi_{JM_J} = E\Psi_{JM_J}, \quad (21)$$

with the help of the Rayleigh-Ritz variational principle. The matrix elements of Hamiltonian can be easily obtained if all the orbital angular momenta are zero, which is reasonable for only considering the low-lying states of five-quark system. It is worthwhile to mention that if the orbital angular momenta of the system are not zero, it is necessary to use the infinitesimally shifted Gaussian method to calculate the matrix elements [36].

3 Results and discussions

In this section, we present the calculation results of all low-lying states of the $(uuc)(s\bar{c})$, $(uus)(c\bar{c})$ and $(usc)(u\bar{c})$ five-quark system with all possible quantum numbers $IJ^P = 0(\frac{1}{2})^-, 0(\frac{3}{2})^-, 0(\frac{5}{2})^-, 1(\frac{1}{2})^-, 1(\frac{3}{2})^-$ and $1(\frac{5}{2})^-$ in ChQM. All the orbital angular momentum of the system is treated as zero and the corresponding parity is negative. In addition, a stability method to identify genuine resonance states, real-scaling method [39,40,41], is employed. In this method, the Gaussian size parameter r_n for the basis functions between baryon and meson clusters for the color-singlet channels is scaled by multiplying a factor α : $r_n \rightarrow \alpha r_n$. As a result, a genuine resonance will act as an avoid-crossing structure (see Fig. 1) with the increasing of α , while other continuum states will fall off towards its threshold. If the avoid-crossing structure is repeated periodically as α increase, then the avoid-crossing structure is a genuine resonance [42].

In Tables III, IV and V, the important calculation results are shown. In each table, columns 2 to 5 represent flavor, spin and color each wave functions in each channel and the corresponding physical channel of five-quark system. In column 6, the eigen-energy of the each

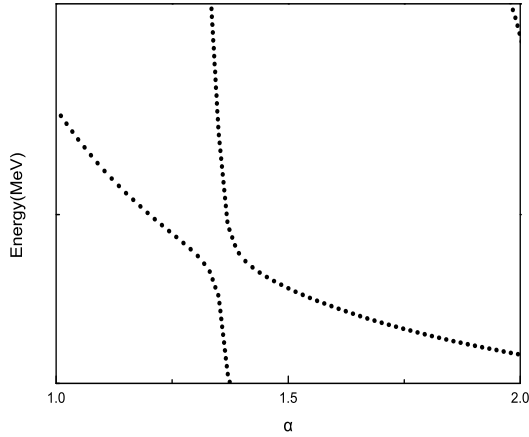


Fig. 1 The shape of the resonance in real-scaling method

channel is listed and the theoretical threshold (the sum of the theoretical masses of corresponding baryon and meson) is given in column 7. Column 8 gives the binding energies, which are the difference between the eigenenergy and the theoretical threshold. Finally, the experimental thresholds (the sum of the experimental masses of the corresponding baryon and meson) along with corrected energies (the sum of experimental threshold and the binding energy, $E' = E_B + E_{th}^{exp}$) are given in last two columns. With this correction, the calculation error caused by the model parameters in five-quark calculation can be reduced partly.

Since we hardly found any bound state in the quantum number of $I = 1$ systems, we do not present the results of these systems but focused our analysis on systems with $IJ^P = 0\frac{1}{2}^-$, $IJ^P = 0\frac{3}{2}^-$ and $IJ^P = 0\frac{5}{2}^-$. The results are analyzed in the following:

(a) For $IJ^P = 0\frac{1}{2}^-$ system in Table III: First, the single channel calculations show that there exist weakly bound states in the $\Xi_c D$, $\Xi_c D^*$ and $\Xi'_c D$ channels. After coupling to respective hidden-color channels, the attractions all increase by a few MeVs, which is the typical range of binding energy of hadronic molecules. The coupling of all color singlet-singlet channels does not push the lowest energy of $\Lambda\eta_c$ below its threshold. Then, a full-channel coupling is made and the results show no bound state can be formed. However, resonances are possible because the attractions exist in the $\Xi_c D$, $\Xi_c D^*$ and $\Xi'_c D$ channels. Thus, real-scaling method is required to identify resonances.

(b) For $IJ^P = 0\frac{3}{2}^-$ system in Table IV: The single channel calculation results show there are weakly bound states in three single channels, $\Xi_c D^*$, $\Xi'_c D^*$ and $\Xi_c^* D$. Moreover, their respective hidden-color channels

increase their attraction a little. No bound state can be obtained in the color singlet-singlet and full channel coupling calculations. Resonances are still possible.

(c) For $IJ^P = 0\frac{5}{2}^-$ system in Table V, there is only one color singlet-singlet channel ($\Xi_c^* D^*$) and there exist a bound state with binding energy ~ 5 MeV. Generally attractions exist between two vector hadrons, and the energy of the system is higher than the sum of two pseudoscalar mesons, resonances are always expected here because of the high angular momentum of the state, which make the coupling between vector-vector mesons channel and pseudoscalar-pseudoscalar mesons channel via the tensor interaction. Thus, $\Xi_c^* D^*$ can be a good candidate for pentaquark and more experimental data are needed in the future.

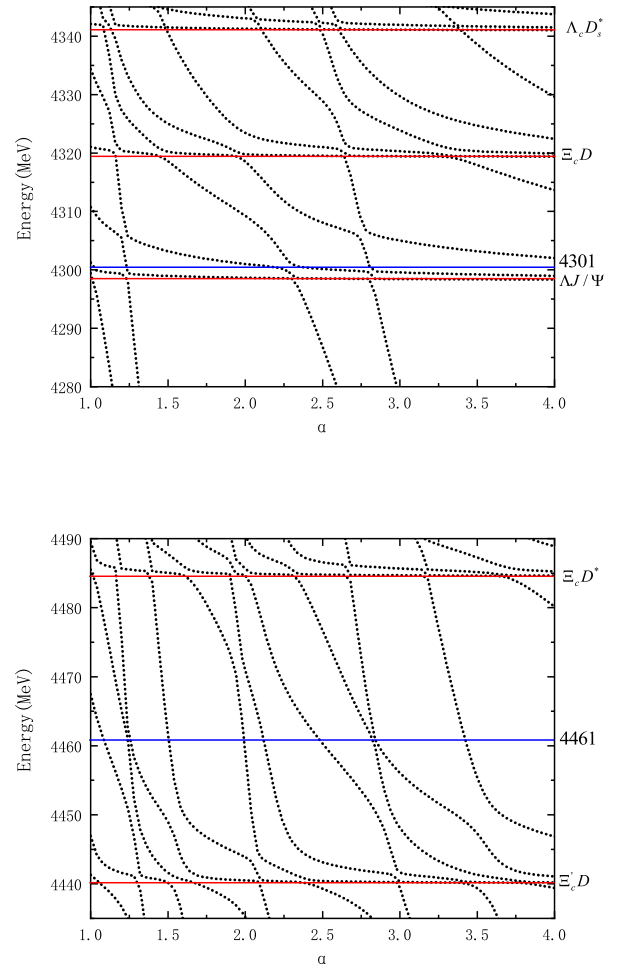


Fig. 2 Energy spectrum of $0\frac{1}{2}^-$ system.

To check whether the resonances with quantum numbers $IJ^P = 0\frac{1}{2}^-$, $0\frac{3}{2}^-$ can survive after coupling to

Table 3 The results for $IJ^P = 0\frac{1}{2}^-$. cc1: mixing of color singlet-singlet channels, cc2: mixing of all channels. (unit: MeV)

Index	ψ^{f_i}	ψ^{σ_j}	ψ^{c_k}	Physical channel	E	E_{th}^{theo}	E_B	E_{th}^{exp}	E'
1	$i = 1$	$j = 2$	$k = 1$	$\Lambda\eta_c$	4098	4098	0	4100	4100
2	$i = 1$	$j = 1, 2$	$k = 1, 2, 3$		4098				
3	$i = 1$	$j = 4$	$k = 1$	$\Lambda J/\psi$	4296	4296	0	4213	4213
4	$i = 1$	$j = 3, 4$	$k = 1, 2, 3$		4296				
5	$i = 2$	$j = 2$	$k = 1$	$\Lambda_c D_s$	4148	4148	0	4250	4250
6	$i = 2$	$j = 1, 2$	$k = 1, 2, 3$		4148				
7	$i = 2$	$j = 4$	$k = 1$	$\Lambda_c D_s^*$	4340	4340	0	4398	4398
8	$i = 2$	$j = 3, 4$	$k = 1, 2, 3$		4340				
9	$i = 3$	$j = 2$	$k = 1$	$\Xi_c D$	4313	4318	-5	4335	4330
10	$i = 3$	$j = 1, 2$	$k = 1, 2, 3$		4312		-6		4329
11	$i = 3$	$j = 4$	$k = 1$	$\Xi_c D^*$	4480	4483	-3	4478	4475
12	$i = 3$	$j = 3, 4$	$k = 1, 2, 3$		4478		-5		4473
13	$i = 4$	$j = 1$	$k = 1$	$\Xi'_c D$	4436	4439	-3	4443	4440
14	$i = 4$	$j = 1, 2$	$k = 1, 2, 3$		4435		-4		4439
15	$i = 4$	$j = 3$	$k = 1$	$\Xi'_c D^*$	4604	4604	0	4586	4586
16	$i = 4$	$j = 3, 4$	$k = 1, 2, 3$		4604				
17	$i = 4$	$j = 5$	$k = 1$	$\Xi_c D^*$	4676	4676	0	4652	4652
18	$i = 4$	$j = 5$	$k = 1, 2, 3$		4676				
cc1					4098		0		
cc2					4098				

Table 4 The results for $IJ^P = 0\frac{3}{2}^-$. cc1: mixing of color singlet-singlet channels, cc2: mixing of all channels. (unit: MeV)

Index	ψ^{f_i}	ψ^{σ_j}	ψ^{c_k}	Physical channel	E	E_{th}^{theo}	E_B	E_{th}^{exp}	E'
1	$i = 1$	$j = 7$	$k = 1$	$\Lambda J/\psi$	4296	4296	0	4213	4213
2	$i = 1$	$j = 6, 7$	$k = 1, 2, 3$		4296				
3	$i = 2$	$j = 7$	$k = 1$	$\Lambda_c D_s^*$	4340	4340	0	4398	4398
4	$i = 2$	$j = 6, 7$	$k = 1, 2, 3$		4340				
5	$i = 3$	$j = 7$	$k = 1$	$\Xi_c D^*$	4481	4483	-2	4478	4476
6	$i = 3$	$j = 6, 7$	$k = 1, 2, 3$		4480		-3		4475
7	$i = 4$	$j = 7$	$k = 1$	$\Xi'_c D^*$	4600	4604	-4	4586	4582
8	$i = 4$	$j = 6, 7$	$k = 1, 2, 3$		4599		-5		4581
9	$i = 4$	$j = 8$	$k = 1$	$\Xi_c^* D$	4510	4511	-1	4509	4508
10	$i = 4$	$j = 8$	$k = 1, 2, 3$		4510		-1		4508
11	$i = 4$	$j = 9$	$k = 1$	$\Xi_c^* D^*$	4676	4676	0	4652	4652
12	$i = 4$	$j = 9$	$k = 1, 2, 3$		4676				
cc1					4296		0		
cc2					4296				

Table 5 The channels with $IJ^P = 0\frac{5}{2}^-$.

Index	ψ^{f_i}	ψ^{σ_j}	ψ^{c_k}	Physical channel	E	E_{th}^{theo}	E_B	E_{th}^{exp}	E'
1	$i = 4$	$j = 10$	$k = 1$	$\Xi_c^* D^*$	4672	4676	-4	4652	4648
2	$i = 4$	$j = 10$	$k = 1, 2, 3$		4671		-5		4647

the open channels, the real-scaling method is employed. The results are shown in Figs. 2, 3 and 4. In these figures, the thresholds of all physical channels appear as horizontal lines and are marked with lines (red lines), tagged with their contents. And for genuine resonances, which appear as avoid-crossing structure and are marked with blue lines. The continuum states fall off towards their respective threshold states (red horizontal lines).

For $IJ^P = 0\frac{1}{2}^-$ system, we get two resonances whose energy are 4301 MeV (main component is $\Xi_c D$) and 4461 MeV (main component is $\Xi_c D^*$). Especially for $P_{cs}(4461)$, which is very close to 4459 MeV, it is a good

candidate for $P_{cs}(4459)$ reported by LHCb Collaboration. In $IJ^P = 0\frac{3}{2}^-$ system, there are three resonances, $P_{cs}(4443)$ (main component is $\Xi_c D^*$), $P_{cs}(4500)$ (main component is $\Xi_c^* D$) and $P_{cs}(4601)$ (main component is $\Xi'_c D^*$). Finally, in $IJ^P = 0\frac{5}{2}^-$ system, there is only one bound state marked horizontally under its threshold ($P_{cs}(4671)$), it will turn to a narrow resonance state after coupling to $\Xi_c D$ via tensor interaction.

It is worth mentioning that in case we use real-scaling method to identify resonances, we will also calculate the composition of the possible resonances to find the mechanism of the formation the resonances.

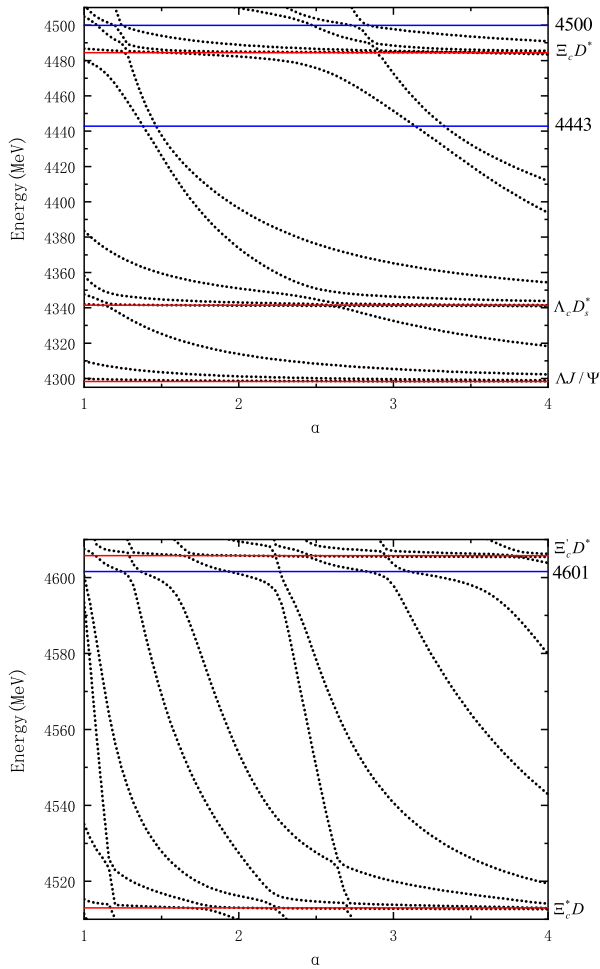


Fig. 3 Energy spectrum of $0_{\frac{3}{2}}^-$ system.

The main component of a genuine resonance should be bound state channels in the single channel or coupling channel (the main component channel and other channels with energies higher than the main component channel) calculations. In Figs. 2, 3, in addition to the resonances found, there are other avoid-crossing structures such as 4306 MeV in $IJ^P = 0_{\frac{1}{2}}^-$ system and 4525 MeV in $IJ^P = 0_{\frac{3}{2}}^-$ system. However, their components are open channels, which means the avoid-crossing structures are formed due to the difference in the decay slope of different open channels.

For resonances, the partial widths of two mesons strong decay can be extracted from these figures. The decay width of resonance to possible open channels of two mesons is obtained by the following formula

$$\Gamma = 4V(\alpha) \frac{\sqrt{(k_r \times k_c)}}{|k_r - k_c|}, \quad (22)$$

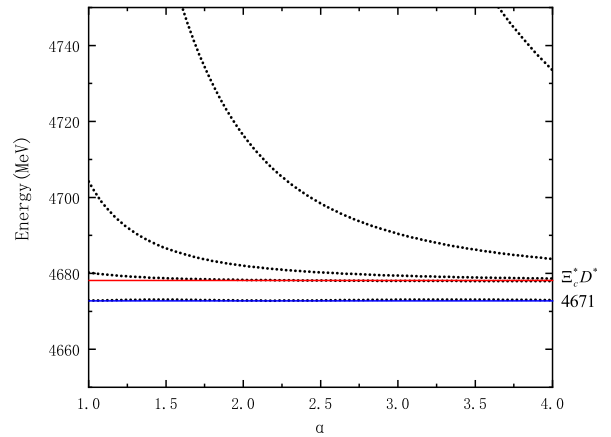


Fig. 4 Energy spectrum of $0_{\frac{5}{2}}^-$ system.

where $V(\alpha)$ is the minimum energy difference, while k_c and k_r stand for the slopes of scattering state and resonance state respectively. More details can be found in Ref. [39].

To extract the partial decay to specific channel, more calculations are needed. For example, to obtain the partial decay width of resonance $P_{cs}(4461)$ in $IJ^P = 0_{\frac{1}{2}}^-$ system, the channel coupling calculations with three bound state channels, $\Xi_c D$, $\Xi_c D^*$ and $\Xi_c' D$ and one of four open channels: $\Lambda \eta_c$, $\Lambda J/\psi$, $\Lambda_c D_s$, and $\Lambda_c D_s^*$ are performed, the results are shown in Fig. 5. From Fig. 5(a), one can extract the partial decay width of $P_{cs}(4461)$ to $\Lambda \eta_c$ and so on. In different channel coupling calculations, the obtained resonance energies are slightly different, from 4453 MeV to 4458 MeV. It is due to the finite model space used, the avoid-crossing structures appear at different scaling factors. Finally, all possible resonances and their respective partial decay widths and total decay width to two ground hadrons are shown in the Table VI and VII. The main component of each resonance and corrected energy are also given in the tables.

From Tables 6-7, we can see that, in $0_{\frac{1}{2}}^-$ system, the total decay width of $P_{cs}(4301)$ is 4.0 MeV and we found its decay width to channel $\Lambda \eta_c$ is very narrow. However, we found no typical avoid-crossing structures when we calculated its decay width to channel $\Lambda_c D_s$, which is a problem that needs further study. For $P_{cs}(4461)$, the decay width is 8.9 MeV and $\Lambda \eta_c$ is the main decay channel. In $0_{\frac{3}{2}}^-$ system, the decay width of two resonances $P_{cs}(4500)$ and $P_{cs}(4601)$ are 7.3 MeV and 5.9 MeV, the main decay channel of $P_{cs}(4500)$ is $\Lambda_c D_s^*$, and $P_{cs}(4601)$ has comparable decay widths to $\Lambda_c D_s^*$ and $\Lambda J/\psi$. For $P_{cs}(4443)$, the decay width is 24.4 MeV and its main de-

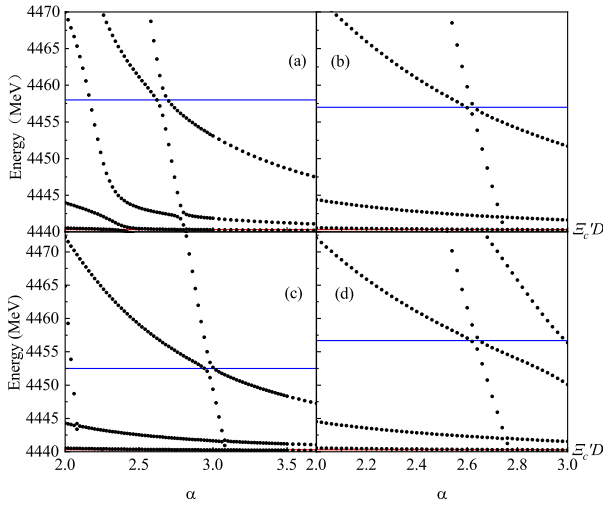


Fig. 5 Energy spectrum of $P_{cs}(4461)$ in four channels coupling, three bound state channels: $\Xi_c D$, $\Xi_c D^*$ and $\Xi_c' D$, and one open channel for $0\frac{1}{2}^-$ system. The open channel is (a) $A\eta_c$, (b) AJ/ψ , (c) $\Lambda_c D_s$, and (d) $\Lambda_c D_s^*$.

Table 6 The decay width of P_{cs} states in $0\frac{1}{2}^-$ system (unit: MeV).

Mode	$P_{cs}(4301)$	$P_{cs}(4461)$
Total Width	4.0	8.9
$A\eta_c$	2.5	3.7
AJ/ψ	1.5	1.2
$\Lambda_c D_s$?	1.5
$\Lambda_c D_s^*$	—	2.5
Main Comp.	$\Xi_c D$	$\Xi_c D^*$
E'	4318	4458

Table 7 The decay width of P_{cs} states in $0\frac{3}{2}^-$ system (unit: MeV).

Mode	$P_{cs}(4443)$	$P_{cs}(4500)$	$P_{cs}(4601)$
Total Width	24.4	7.3	5.9
AJ/ψ	19.6	1.7	3.3
$\Lambda_c D_s^*$	4.8	5.6	2.6
Main Comp.	$\Xi_c D^*$	$\Xi_c^* D$	$\Xi_c' D^*$
E'	4444	4497	4585

channel is AJ/ψ . For $0\frac{3}{2}^-$ system, there is only resonance $P_{cs}(4671)$, which is 5 MeV under its threshold and the decay width is estimated to be 5-15 MeV due to decay widths of its constituents, Ξ_c^* ($\Gamma_{\Xi_c^* \rightarrow \Xi_c \pi} \sim 2.35$ MeV) and D^* ($\Gamma_{D^* \rightarrow D \pi} \sim 2$ MeV) and the decay width to $\Xi_c D$, 1 ~ 10 MeV, via tensor interaction. Considering the deviation of quark model calculations and the uncertainty of experimental results, $P_{cs}(4461)$ in $0\frac{1}{2}^-$ system can be identified as $P_{cs}(4459)$ reported by LHCb Collaboration.

4 Summary

In this paper, the hidden-charm pentaquark systems with single strangeness is investigated in chiral quark model. The calculation shows that there are several states in systems $0\frac{1}{2}^-$, $0\frac{3}{2}^-$ and $0\frac{5}{2}^-$, which means good resonances can be formed. Real-scaling method are used to check the genuine resonances and study their decay width. In $0\frac{1}{2}^-$ system, two resonances $P_{cs}(4301)$ and $P_{cs}(4461)$ have been found. In particular, $P_{cs}(4461)$, whose main component is $\Xi_c D^*$, is regarded as a good candidate for $P_{cs}(4459)$ recently reported by LHCb Collaboration. Other possible pentaquarks are also predicted. Three states, $P_{cs}(4443)$, $P_{cs}(4500)$ and $P_{cs}(4601)$ are found in system $0\frac{3}{2}^-$. It is worth mentioning that there are $P_{cs}(4461)$ and $P_{cs}(4443)$ in our calculations, which can form a two-peak structure composed of $\Xi_c D^*$ states with quantum number of $0\frac{1}{2}^-$ and $0\frac{3}{2}^-$, similar to $P_c(4440)$ and $P_c(4457)$. Finally, only one molecule state $\Xi_c^* D^*$ exists in system $0\frac{5}{2}^-$ and it is a good candidate for heavy pentaquark with high spin with its decay width is in range of 5 MeV to 15 MeV.

From the results, one can see that the behaviors of P_{cs} systems are similar to that of P_c systems. Due to the success of chiral quark model on P_c states [32], it is expected that the possible resonances proposed above can be searched in future experiments.

Acknowledgments

The work is supported partly by the National Natural Science Foundation of China under Grant Nos. 11775118, and 11535005.

References

1. D. Diakonov, V. Petrov and M. Polyakov, Z. Phys. A 359, 305 (1997).
2. T. Nakano et al. [LEPS Collaboration], Phys. Rev. Lett. 91, 012002 (2003).
3. R. Aaij et al. [LHCb Collaboration], Phys. Rev. Lett. 115, 072001 (2015).
4. R. Aaij et al. [LHCb Collaboration], Phys. Rev. Lett. 122, 222001 (2019).
5. R. Chen, X. Liu and S. L. Zhu, Nucl. Phys. A 954, 406-421(2016).
6. H. X. Chen, E. L. Cui, W. Chen, X. Liu, T. G. Steele and S. L. Zhu, Eur. Phys. J. C 76, 572 (2016).
7. Z. G. Wang, Eur. Phys. J. C 76, 70 (2016).
8. Q. F. Lu and Y. B. Dong, Phys. Rev. D 93, 074020 (2016).
9. J. He, Eur. Phys. J. C 79, 393 (2019).
10. M. Z. Liu, Y. W. Pan, F. Z. Peng, and M. S. Sánchez, L. S. Geng, A. Hosaka, and M. P. Valderrama, Phys. Rev. Lett. 122, 242001 (2019).

11. C. J. Xiao, Y. Huang, Y. B. Dong, L. S. Geng, and D. Y. Chen, *Phys. Rev. D* 100, 014022 (2019).
12. L. Maiani, A. D. Polosa and V. Riquer, *Phys. Lett. B* 749, 289 (2015).
13. C. R. Deng, J. L. Ping, H. X. Huang and F. Wang, *Phys. Rev. D* 95, 014031 (2017).
14. C.-J. Xiao, Y. Huang, Y.-B. Dong, L. S. Geng, and D.-Y. Chen, *Phys. Rev. D* 100, 014022 (2019).
15. R. Aaij et al. [LHCb Collaboration], arXiv:2012.10380 [hep-ex].
16. H. X. Chen, W. Chen, X. Liu and X. H. Liu, [arXiv:2011.01079 [hep-ph]].
17. Z. G. Wang, arXiv:2011.05102[hep-ph].
18. C. W. Xiao, J. J. Wu and B. S. Zou, *Phys.Rev. D* 103, 054016 (2021).
19. F. Z. Peng, M. J. Yan, M. S. Sánchez and M. P. Valderama, arXiv:2011.01915 [hep-ph].
20. Rui Chen, *Eur. Phys. J. C* 81, 122 (2021).
21. W. Y. Liu, W. Hao, G. Y. Wang, Y. Y. Wang and E. Wang, *Phys.Rev. D* 103, 034019 (2021)
22. Rui Chen, *Phys.Rev. D* 103, 054007 (2021)
23. Jun-Tao Zhu, Lin-Qing Song and Jun He, *Phys.Rev. D* 103, 074007 (2021).
24. K. Azizi, Y. Sarac and H. Sundu, *Phys.Rev. D* 103, 094033 (2021).
25. A. Feijoo, V. K. Magas, A. Ramos and E. Oset, *Eur. Phys. J. C* 76, 446 (2016).
26. J. X. Lu, E. Wang, J. J. Xie, L. S. Geng and E. Oset, *Phys. Rev. D* 93, 094009 (2016).
27. H. X. Chen, L. S. Geng, W. H. Liang, E. Oset, E. Wang and J. J. Xie, *Phys. Rev. C* 93, 065203 (2016).
28. B. Wang, L. Meng and S. L. Zhu, *Phys. Rev. D* 101, 034018 (2020).
29. J. J. Wu, R. Molina, E. Oset and B. S. Zou, *Phys. Rev. Lett.* 105, 232001 (2010).
30. J. J. Wu, R. Molina, E. Oset and B. S. Zou, *Phys. Rev. C* 84, 015202 (2011).
31. Z. C. Yang, Z. F. Sun, J. He, X. Liu, and S. L. Zhu, *Chin. Phys. C* 36, 6 (2012).
32. H. X. Huang and J. L. Ping, *Phys. Rev. D* 99, 014010 (2019).
33. C. J. Xiao, Y. Huang, Y. B. Dong, L. S. Geng, and D. Y. Chen, *Phys. Rev. D* 100, 014022 (2019).
34. M. Gell-Mann, *Phys. Lett.* 8, 214 (1964).
35. G. Zweig, CERN-TH-412 (2020).
36. E. Hiyama, Y. Kino, M. Kamimura, *Prog. Part. Nucl. Phys.* 51, 223 (2003).
37. A. Valcarce, H. Garcilazo, F. Fernandez, P. Gonzalez, *Rep. Prog. Phys.* 68, 965 (2005)
38. J. Vijande, F. Fernandez, A. Valcarce, *J. Phys. G* 31, 481 (2005)
39. J. Simons, *J. Chem. Phys.* 75, 2465 (1981)
40. E. Hiyama, A. Hosaka, M. Oka, J. M. Richard, *Phys. Rev. C* 98, 045208 (2018)
41. Q. Meng, E. Hiyama, K.U. Can, P. Gubler, M. Oka, A. Hosaka, H. Zong, *Phys. Lett. B* 798, 135028 (2019)
42. Y. Tan, J. L. Ping, *Chin. Phys. C* 45, 093104 (2021).